

Sets of FCS experiments to quantify free diffusion coefficients in reaction-diffusion systems. The case of Ca^{2+} and its dyes

Lorena Sigaut, Cecilia Villarruel, María Laura Ponce and Silvina Ponce Dawson

*Departamento de Física, FCEN-UBA, and IFIBA, CONICET,
Ciudad Universitaria, Pabellón I, (1428) Buenos Aires, Argentina*

Abstract

Many cell signaling pathways involve the diffusion of *messengers* that bind/unbind to intracellular components. Quantifying their net transport rate under different conditions, then requires having separate estimates of their free diffusion coefficient and binding/unbinding rates. In this paper, we show how performing sets of *Fluorescence Correlation Spectroscopy* (FCS) experiments under different conditions, it is possible to quantify free diffusion coefficients and on and off rates of reaction-diffusion systems. We develop the theory and present a practical implementation for the case of the universal second messenger, calcium (Ca^{2+}) and single-wavelength dyes that increase their fluorescence upon Ca^{2+} binding. We validate the approach with experiments performed in aqueous solutions containing Ca^{2+} and Fluo4 dextran (both in its High and Low Affinity versions). Performing FCS experiments with tetramethylrhodamine-dextran in *Xenopus laevis* oocytes, we infer the corresponding free diffusion coefficients in the cytosol of these cells. Our approach can be extended to other physiologically relevant reaction-diffusion systems to quantify biophysical parameters that determine the dynamics of various variables of interest.

I. INTRODUCTION

Many cell signaling pathways involve the diffusion of messengers in the cytoplasm. In most cases these substances convey their message by binding to target molecules. Furthermore, as they reach their targets they not only diffuse freely but also bind/unbind to other cell components. For long enough times, the net transport that results from the combination of free diffusion and binding/unbinding is described by *effective diffusion coefficients* that are weighted averages of the free coefficients of the messenger and of the substance it interacts with that depend on their concentrations and reaction rates. The universal second messenger calcium (Ca^{2+}) provides a prototypical example of this behavior. Persistently high cytosolic Ca^{2+} concentrations lead to cell death. For this reason cells have numerous mechanisms to reduce this concentration, the fastest one of which is *buffering*. Buffers are molecules that bind/unbind to/from Ca^{2+} ions reducing their free concentration. In doing so they also alter the spatio-temporal cytosolic Ca^{2+} distribution [1], [2] and the effect of the resulting signals on the eventual end responses [3]. This means that the time and spatial range of action of Ca^{2+} as messenger is strongly dependent on the Ca^{2+} concentration itself. There is a large variety of intracellular Ca^{2+} signals ranging from those that arise upon the opening of a single Ca^{2+} channel on the plasma membrane or on the membrane of intracellular stores to those that manifest themselves as Ca^{2+} waves that travel throughout the whole cell [4]. This in turn implies that the cytosolic Ca^{2+} concentration attains very different values depending on the signal type. The resulting Ca^{2+} effective diffusion coefficient then varies across disparate values depending on the signal type. The range of values was estimated to be $\sim [5, 220] \mu m^2/s$ [5] with increasing values as the cytosolic Ca^{2+} concentration increased. How fast can Ca^{2+} diffuse inside cells? In order to answer this question it is necessary to have separate estimates of the Ca^{2+} and Ca^{2+} buffers free diffusion coefficients, their concentrations and reactions rates. Ideally, having access to this information one could eventually compute the Ca^{2+} effective diffusion coefficient as a function of its concentration. One could wonder why having access to this information would be necessary to study Ca^{2+} signals. After all, they can be observed in intact cells using Ca^{2+} dyes. The Ca^{2+} dye fluorescence, however, provides information on the Ca^{2+} -bound dye concentration which distribution depends on the dye kinetic and transport properties. In particular, Ca^{2+} signals that are evoked via the photo-release of caged compounds with UV light are imaged using

single wavelength dyes that increase their fluorescence when bound to Ca^{2+} [6], [7]. It was shown in Bruno et al., 2010 [8] that Ca^{2+} current estimates inferred from images that use such dyes are quite sensitive to uncertainties in the on rate of the Ca^{2+} -dye binding reaction and in the diffusion coefficient of the dye, two parameters that are usually poorly known. Having reliable estimates of these parameters is thus unavoidable to extract quantitative information from images of Ca^{2+} signals and allow the effective interplay between modeling and experiment that is necessary to attain a comprehensive description of the signals. In this paper we describe and implement an approach that shows how performing sets of *Fluorescence Correlation Spectroscopy* (FCS) [9] experiments under different conditions and using a reaction-diffusion model to interpret the experimental results it is possible to obtain separate estimates of these key biophysical parameters.

In FCS the fluorescence intensity in a small volume is recorded along time and, via an analysis of the temporal autocorrelation of the observed fluctuations, the transport rates of the fluorescent species are, in principle, derived [10]. FCS has been widely used to determine the diffusion coefficients of fluorescently labeled proteins inside cells [11], [12], [13]. When the fluorescent species diffuse freely in medium there is an analytic expression for the autocorrelation function of the fluorescent fluctuations (ACF) that is used to fit the experimental observations and derive diffusion coefficients (see Materials and Methods). When the fluorescent particles diffuse and react, simple analytic expressions for the ACF can only be obtained under certain approximations [13], [14], [15], [16]. In particular, we have shown in Sigaut et al., 2010 [16] (see also [14], [15]), that when the reactions occur on a somewhat faster timescale than diffusion the correlation time of the fluctuations is determined by the effective diffusion coefficients mentioned before. Our theoretical studies showed that information on reaction rates could also be derived from the fitting [14], [16]. In this paper we present a practical implementation of such an approach in which the experimental conditions are changed so as to maximize the information that can be drawn from the data. More specifically, we do it for the case of Ca^{2+} and single wavelength Ca^{2+} dyes. This case shares some common features with the case in which proteins diffuse and react, but it differs slightly since fluctuations are also due to changes in fluorescence intensity associated to the Ca^{2+} -dye binding/unbinding reaction. This requires the development of a new theoretical framework that we introduce in this paper as well.

In order to advance with the practical implementation presented here we first study

theoretically the behavior of the ACF for a case with Ca^{2+} and a single wavelength dye. We derive an analytic approximation under the assumption that the Ca^{2+} -dye reaction occurs on a fast timescale. We compare this approximated ACF with the one without approximations computed numerically and determine the range of parameter values for which the approximated ACF can give reasonable estimates of certain parameters. We then show the results of a series of FCS experiments performed in aqueous solutions containing Ca^{2+} and different amounts of the Ca^{2+} indicator Fluo4 dextran both in its High and Low Affinity versions (Invitrogen-Molecular Probes, Carlsbad, CA). Fitting the observed ACF by the analytic approximation we corroborate the validity of the approximations and derive diffusion coefficients and the off-rate of the Ca^{2+} -dye binding reaction, in solution. A similar approach can be used to characterize the kinetic properties of other Ca^{2+} dyes. Even if the free diffusion coefficients in solution and in the cytosol are different due to differences in viscosity between both media, we may assume that the ratio between the free diffusion coefficients of any two substances remains the same in both settings. This is particularly relevant, because by solely quantifying the rate of diffusion of a molecule that diffuses freely in the cytosol and in solution we can infer the free diffusion coefficient of Ca^{2+} and the dyes in the cytosol as well. We present such quantification in the Appendix. Thus, the practical implementation presented in this paper not only highlights the advantages of our approach but it also allows us to derive information that is key to quantify the free Ca^{2+} distribution that underlies a Ca^{2+} image.

Ca^{2+} signals are not the only example in which being able to tell apart the contributions of free diffusion and reactions on the net transport rate of labeled substances is relevant. We have recently shown [17] the necessity of going beyond the description of effective coefficients to interpret correctly the apparently disparate estimates of the protein, Bicoid, diffusion coefficient derived from FCS [18] and Fluorescence Recovery After Photobleaching (FRAP) [19] experiments. This example also shows that the comprehensive quantifiable description of a physiological process requires having a biophysical model for the dynamics of the relevant concentrations that depends on concentration-independent biophysical parameters. It is via such a model that the response of the system over time in front of different stimuli can be predicted. Being able to derive estimates of the concentration-free biophysical parameters *in situ* is thus relevant to achieve a meaningful description. The approach presented in this paper can be adapted and applied to other problems. Therefore,

its relevance goes beyond quantifying the biophysical parameters associated to Ca^{2+} and its dyes.

II. MATERIALS AND METHODS

A. FCS Theory

Fluorescence Correlation Spectroscopy (FCS) monitors the fluctuation of the fluorescence in a small volume. Fluctuations are characterized by the time-averaged autocorrelation function (ACF) which is defined as:

$$G(\tau) = \frac{\langle \delta f(t) \delta f(t + \tau) \rangle}{\langle f(t) \rangle^2} \quad (1)$$

where $\langle f(t) \rangle$ is the average fluorescence in the sampling volume and $\delta f(t)$ is the deviation with respect to this mean at each time, t . As explained in the Appendix, when the fluorescence comes from a single species, P_f , that diffuses freely with coefficient D_f (i.e., does not react) the ACF is of the form:

$$G(\tau) = \frac{Go}{\left(1 + \frac{\tau}{\tau_f}\right) \sqrt{1 + \frac{\tau}{w^2 \tau_f}}} \quad (2)$$

where $w = w_z/w_r$ is the aspect ratio of the sampling volume and w_z and w_r are the sizes of the beam waist along z and r , with z the spatial coordinate along the beam propagation direction and r a radial coordinate in the perpendicular plane; the effective volume is $V_{ef} \equiv \pi^{3/2} w_r^2 w_z$; $\tau_f = w_r^2/(4D_f)$ is the characteristic time of diffusion of the particles across the sampling volume and $Go = G(\tau = 0) = 1/(V_{ef} P_{tot})$, where P_{tot} is the particle concentration. When the dynamics of the fluorescent species is described by a reaction-diffusion model most often there is not a simple analytic expression for the ACF. It can always be written as a sum of integrals each one associated to one of the branches of eigenvalues that rule the dynamics of the linearized reaction-diffusion equations of the model. Each of these integrals is called a “component” of the ACF. In the case of interest for the present paper there are three relevant species: free Ca^{2+} (Ca), free dye (F) and Ca^{2+} -bound dye (CaF), which diffuse with free coefficients D_{Ca} (Ca), and D_F (F and CaF) and react according to:



with on- and off-rates, k_{on} and k_{off} respectively. The corresponding (spatially uniform) equilibrium concentrations, Ca_{eq} , F_{eq} and CaF_{eq} satisfy:

$$CaF_{eq} = \frac{Ca_{eq}F_{tot}}{Ca_{eq} + K_d} \quad (4)$$

where $K_d = k_{off}/k_{on}$ and $F_{tot} = F_{eq} + CaF_{eq}$ is the total dye concentration. There are three branches of eigenvalues for this system and the ACF then has three components. Simple algebraic expressions can be obtained for the components in certain limits. In particular, in this paper we present the results obtained in the “fast reaction limit” that holds when the characteristic time of the reaction Eq. (3) is shorter than the time it takes for the species to diffuse across the observation volume (i.e., if $\tau_{reac} \equiv (k_{off} + k_{on}(Ca_{eq} + F_{eq}))^{-1} < w_r^2/(4D_F)$). For more details see the Appendix where we also compare the “full” (integral expression of the) ACF computed numerically with the analytic approximation derived in the fast reaction limit that is presented in the Results Section and some of their components separately.

B. FCS Experiments

1. Aqueous solutions

Aqueous solutions were prepared with different concentrations of the Ca^{2+} indicator Fluo4 dextran High or Low Affinity (Invitrogen- Molecular Probes, Carlsbad, CA), employing the solutions of a Ca^{2+} Calibration Buffer Kit (Invitrogen- Molecular Probes). Each solution contained $4.3 \mu M Ca^{2+}$, 100 mM KCl, 30 mM MOPS, pH 7.2, and different concentrations of the Ca^{2+} indicator ranging from 200 nM to 9 μM and from 400 nM to 20 μM for the Low and High Affinity version, respectively. Four or five separate experiments were performed for each solution. Some of the results were finally discarded as explained later. The solutions that were probed and fitted are listed in Table I.

TABLE I. FCS experiments in aqueous solutions containing Fluo4: Solutions composition.

Aqueous solution $C_{a_{tot}}(nM)$ $F4_{tot}(nM)$		
Fluo4 High Affinity		
1	4285	429
2	4285	857
3	4285	1371
4	4285	1886
5	4285	2571
6	4285	4286
7	4285	9000
8	4285	15000
9	4285	19286
Fluo4 Low Affinity		
10	4285	214
11	4285	429
12	4285	857
13	4285	1114
14	4285	1371
15	4285	1886
16	4285	2571
17	4285	4286
18	4285	9000
All the solutions also contain: 100 mM KCl, 30 mM MOPS at pH 7.2		

2. Acquisition

FCS measurements were performed on a spectral confocal scanning microscope FluoView 1000 (Olympus, Tokyo, Japan), employing a 60x, 1.35 N.A. oil-immersion objective (UP-lanSAPO, Olympus) and a pinhole aperture of 115 μm . Single point measurements at a 50

kHz sampling rate were performed for a total duration of 167 s (equivalently, 8365312 data points) employing a 488 nm line and detecting the fluorescence in the range (500-600) nm. The measurements were performed at $\sim 20 \mu m$ from the coverslip.

3. Data analysis

Experimental ACF's were calculated with a custom-made routine written on the Matlab platform [20]. To this end, each 167 s long record was divided into $N = 1021$, 164 ms long segments containing 2^{13} points each for the experiments in aqueous solutions. The ACF was computed for each of the $N = 1021$ segments from which the average ACF was obtained. Based on the theoretical calculations presented in the Results Section, we fitted the average ACF by an expression of the form

$$G(\tau) = \frac{G_0}{\left(1 + \frac{\tau}{\tau_0}\right) \sqrt{1 + \frac{\tau}{w^2\tau_0}}} + \frac{G_1}{\left(1 + \frac{\tau}{\tau_1}\right) \sqrt{1 + \frac{\tau}{w^2\tau_1}}} + \frac{G_2 e^{-\nu\tau}}{\left(1 + \frac{\tau}{\tau_2}\right) \sqrt{1 + \frac{\tau}{w^2\tau_2}}} \quad (5)$$

where $w = w_z/w_r$ is the aspect ratio of the sampling volume, as before, and the various times are related to diffusion coefficients by $\tau_i = w_r^2/(4D_i)$, $i = 1, 2, 3$, with the beam waist, w_r . Only experiments for which the mean fluorescence in the observation volume remained approximately constant during the whole record were fitted. Experiments for which the average ACF was too noisy were also discarded. In all cases we tried to fit the experiments leaving all 7 parameters of Eq. (5) ($G_0, G_1, G_2, \tau_0, \tau_1, \tau_2, \nu$) free to be fitted. In others we set $G_2 = 0$ and only derived G_0, G_1, τ_0 and τ_1 . Thus, we tried a 3-component and a 2-component fit for each experiment. All fitting parameters were determined for each average ACF via a nonlinear least squares fit using the Matlab built-in function `nlinfit`. In the figures we show the average of the displayed fitting parameters and the average error computed over all the experiments in a given set.

4. Characterization of the confocal volume

The radial beam waist and the aspect ratio were determined to be $w_r = 0.262 - 0.292 \mu m$ and $w = w_z/w_r = 5$ by measuring the translational three-dimensional diffusion of fluorescein (Sigma, St. Louis, MO) in buffer solution pH 9, assuming a diffusion coefficient of $425 \mu m^2/s$ [21]. Thus, the resulting effective volume was $V_{ef} = (0.59 \pm 0.1) \mu m^3$.

III. RESULTS

A. FCS theory for a solution with Ca^{2+} and a single wavelength dye in the limit of fast reactions

Proceeding as described in the Appendix we determine that, in the fast reaction limit for the case of a solution of Ca^{2+} and a dye the ACF of the fluorescence fluctuations can be approximated by the sum of three components of the form:

$$G_{approx}(\tau) = G_F(\tau) + G_{ef1}(\tau) + G_{ef2}(\tau) \quad (6)$$

$$G_F(\tau) = \frac{Go_F}{\left(1 + \frac{\tau}{\tau_F}\right) \sqrt{1 + \frac{\tau}{w^2\tau_F}}} \quad (7)$$

$$G_{ef1}(\tau) = \frac{Go_{ef1}}{\left(1 + \frac{\tau}{\tau_{ef1}}\right) \sqrt{1 + \frac{\tau}{w^2\tau_{ef1}}}} \quad (8)$$

$$G_{ef2}(\tau) = \frac{Go_{ef2}e^{-\nu_F\tau}}{\left(1 + \frac{\tau}{\tau_{ef2}}\right) \sqrt{1 + \frac{\tau}{w^2\tau_{ef2}}}} \quad (9)$$

where $\tau_F = w_r^2/(4D_F)$ and $\tau_{efi} = w_r^2/(4D_{efi})$, $i = 1, 2$, with:

$$D_{ef1} = \frac{D_{Ca} + \alpha D_F}{1 + \alpha} \quad (10)$$

$$D_{ef2} = \frac{\alpha D_{Ca} + D_F}{1 + \alpha} \quad (11)$$

and $\alpha = \frac{F_{eq}^2}{F_{tot}K_d}$ and:

$$\nu_F = k_{off} + k_{on}(F_{eq} + Ca_{eq}) \quad (12)$$

The weights Go_F , Go_{ef1} and Go_{ef2} are given by:

$$Go_F = \frac{1}{V_{ef}F_{tot}} \quad (13)$$

$$Go_{ef1} = \frac{1}{V_{ef}CaF_{eq}} \frac{F_{eq}^2}{F_{tot}K_d} \frac{K_d}{(K_d + F_{eq} + Ca_{eq})} \quad (14)$$

$$Go_{ef2} = \frac{1}{V_{ef}CaF_{eq}} \frac{K_d}{(K_d + F_{eq} + Ca_{eq})} \quad (15)$$

The sum of all the weights is inversely proportional to the concentration of fluorescent particles:

$$Go_{tot} = Go_{ef1} + Go_{ef2} + Go_F = \frac{1}{V_{ef}CaF_{eq}} \quad (16)$$

The sum of the two effective diffusion coefficients satisfies:

$$D_{ef1} + D_{ef2} = D_{Ca} + D_F \quad (17)$$

As in Sigaut et al., 2010 [16], the approximate analytic expression of the ACF given by Eqs. (6)-(9) is always valid for large enough τ . The first term, however, is exact. Thus, we can expect to be able to derive D_F from all FCS experiments. The approximations of Go_{ef1} and Go_{ef2} are valid for the values of τ that are relevant to determine τ_{ef1} and τ_{ef2} from a fit to the experiments if $\tau_{reac} \equiv (k_{off} + k_{on}(Ca_{eq} + F_{eq}))^{-1} \ll w_r^2/(4D_{Ca})$.

B. Fitting parameters from FCS experiments in aqueous solutions with Ca^{2+} and Fluo4 dextran

In this Section we show how we proceed to analyze the experimental data. In particular, we show the results of using Eq. (5) to fit the ACF's obtained from the set of experiments of Table I performed with Fluo4 High and Low Affinity. The fitting parameters are G_0 , G_1 , G_2 , ν and the characteristic times τ_0 , τ_1 and τ_2 from which we derive three diffusion coefficients D_0 , D_1 and D_2 as explained before. Fig. 1 shows the diffusion coefficients obtained in this way as a function of the total concentration of the dye used in the solutions, $F4_{tot}$, for High Affinity (Fig. 1 (a)) and Low Affinity (Fig. 1 (b)) Fluo4. We also plot in these figures the expected free diffusion coefficient of the dye, $D_F=85 \mu m^2/s$ [22], and effective diffusion coefficients, D_{ef1} and D_{ef2} , calculated using Eqs. (10) and (11), with the dissociation constant given by the manufacturer ($K_d=772$ nM for High Affinity and $K_d=2600$ nM for Low Affinity), $D_{Ca}=760 \mu m^2/s$ [23], $D_F=85 \mu m^2/s$ and the total calcium and dye concentrations employed in the solutions.

The identification between the fitting parameters G_0 , D_0 , G_1 , D_1 , G_2 , D_2 , ν , and the seven quantities, G_{oF} , D_F , G_{oef1} , D_{ef1} , G_{oef2} , D_{ef2} , ν_F , of the theoretical formulas Eqs. (6) - (9) is immediate in the case of the last three which correspond to the only component with an exponentially decaying term. For the other quantities it is not difficult to make the correspondence because $D_F < D_{Ca}$ implies that $D_F \leq D_{ef1}$. Furthermore, as may be observed in Fig. 1, there is one diffusion coefficient obtained from the fitting, D_0 , that remains approximately invariant for all the analyzed concentrations. This should correspond to the free diffusion of the dye, D_F , which is concentration independent. In this way we determine that $D_F = (65 \pm 7) \mu\text{m}^2/\text{s}$ in the case of Fluo4 High Affinity and $D_F = (89 \pm 8) \mu\text{m}^2/\text{s}$ in the case of Fluo4 Low Affinity. This is clearer in Fig. 1 (a), and the lowest constant diffusion coefficient can also be identified in Fig. 1 (b). The other two diffusion coefficients obtained from the fitting, D_1 and D_2 , change with the dye concentration. This means that they are effective diffusion coefficients. Making the identifications $D_1 = D_{ef1}$ and $D_2 = D_{ef2}$ we know that their lower and upper limits are the free diffusion coefficients of the dye, D_F , and of calcium, D_{Ca} , respectively. In fact, both D_1 and D_2 are larger than D_0 . Furthermore, in Fig. 1 (a), D_1 decreases with $F4_{tot}$ while D_2 increases similarly to their theoretical counterparts, D_{ef1} and D_{ef2} . This shows the validity of the identification between fitting and model parameters. A similar trend can be observed in Fig. 1 (b) although not as clear as in Fig. 1 (a). In any case, we do make the identification $D_1 = D_{ef1}$ and $D_2 = D_{ef2}$ also in this case. It is remarkable that the obtained results seem reasonable even outside the range of validity of the fast reaction approximation.

We test the validity of the theoretical approximation Eqs. (13) and (16) in Fig. 2. Fig. 2 shows plots of the inverse of G_{oF} as a function of the total dye concentration used in the solutions, $F4_{tot}$, with symbols, together with the expected values given by Eq.(13) using the concentrations used in the solutions and the observation volume derived from the calibration, with curves. The results for High and Low Affinity Fluo4 are shown in Figs. 2 (a) and 2 (d), respectively. The logarithmic scale used in the figures highlights the fact that both the experimental and the theoretical results scale similarly with $F4_{tot}$, i.e., as $1/F4_{tot}$ (see Eq. (13)). If we fit the experimental results using the values, $F4_{tot}$, determined by construction of the solution, the effective volume, V_{ef} , can be obtained from the fitting. Considering the inverse of G_{oF} versus $F4_{tot}$, we found expected values ($V_{ef} = (0.54 \pm 0.08) \mu\text{m}^3$ and $V_{ef} = (0.56 \pm 0.08) \mu\text{m}^3$ for High Affinity and Low Affinity Fluo4, respectively)

that are consistent with the one obtained from the calibration ($V_{ef} = (0.59 \pm 0.1) \mu m^3$).

Another property of the ACF is that the sum of all the weights, Go_{tot} , is inversely proportional to the concentration of Ca^{2+} -bound dye, CaF_{eq} (Eq.(16)). In Figs. 2 (b) and 2 (e) we show plots of the values of the inverse of Go_{tot} obtained from the fitting of the ACF as functions of CaF_{eq} and the expected values according to Eq. (16), for High Affinity and Low Affinity Fluo4, respectively. The linear scaling between both quantities is very good also in this case but there is a mismatch in the ordinate. As before, we can fit the experimental results using the equilibrium values, CaF_{eq} , derived from the concentrations used in the solutions and the dissociation constant provided by the vendor. Considering the inverse of Go_{tot} versus CaF_{eq} and fitting with a linear relation, the effective volume inferred was $(0.23 \pm 0.02) \mu m^3$ for Fluo4 High Affinity and $(0.17 \pm 0.01) \mu m^3$ for the Low Affinity

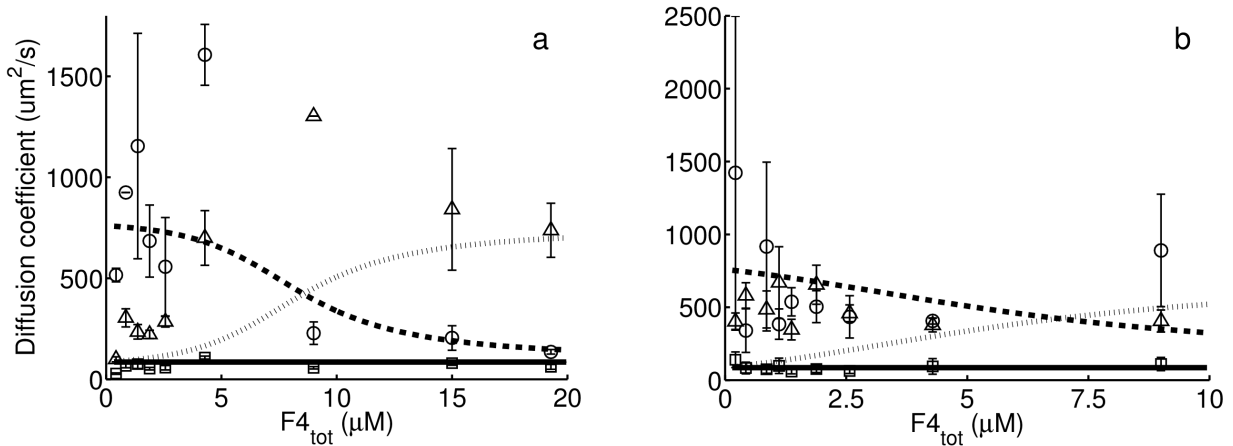


FIG. 1.

Diffusion coefficients obtained from the fitting of the experimental data using Eq. (5), D_0 (squares), D_1 (circles), and D_2 (triangles), as a function of the total calcium dye concentration of the aqueous solutions, $F4_{tot}$. In solid line, $D_F = 85 \mu m^2/s$, and in dash lines expected effective diffusion coefficients, D_{ef1} (bold) and D_{ef2} (light) given by Eqs. (10) and (11) respectively, with the calcium and dye concentrations employed in the aqueous solutions, $D_{Ca} = 760 \mu m^2/s$, $D_F = 85 \mu m^2/s$ and the dissociation constant given by the manufacturer, $K_d = 772$ nM and 2600 nM for High (a) and Low (b) Affinity Fluo4.

version of the dye, which are lower than the one obtained from the calibration ($V_{ef} = (0.59 \pm 0.1) \mu\text{m}^3$).

Finally we show the values of ν_F derived from the fitting and the theoretical curve obtained using the fast reaction approximation, Eqs. (6)-(9), as a function of $F4_{tot}$ for High Affinity (Fig. 2 (c)) and Low Affinity (Fig. 2 (f)) Fluo4. There we observe that the values obtained for low $F4_{tot}$ concentrations are the ones that can be associated to the theoretical expression (Eq. (12)) from which an estimate of k_{off} can be derived. In order to estimate k_{off} however we used all the data available as explained in the Discussion.

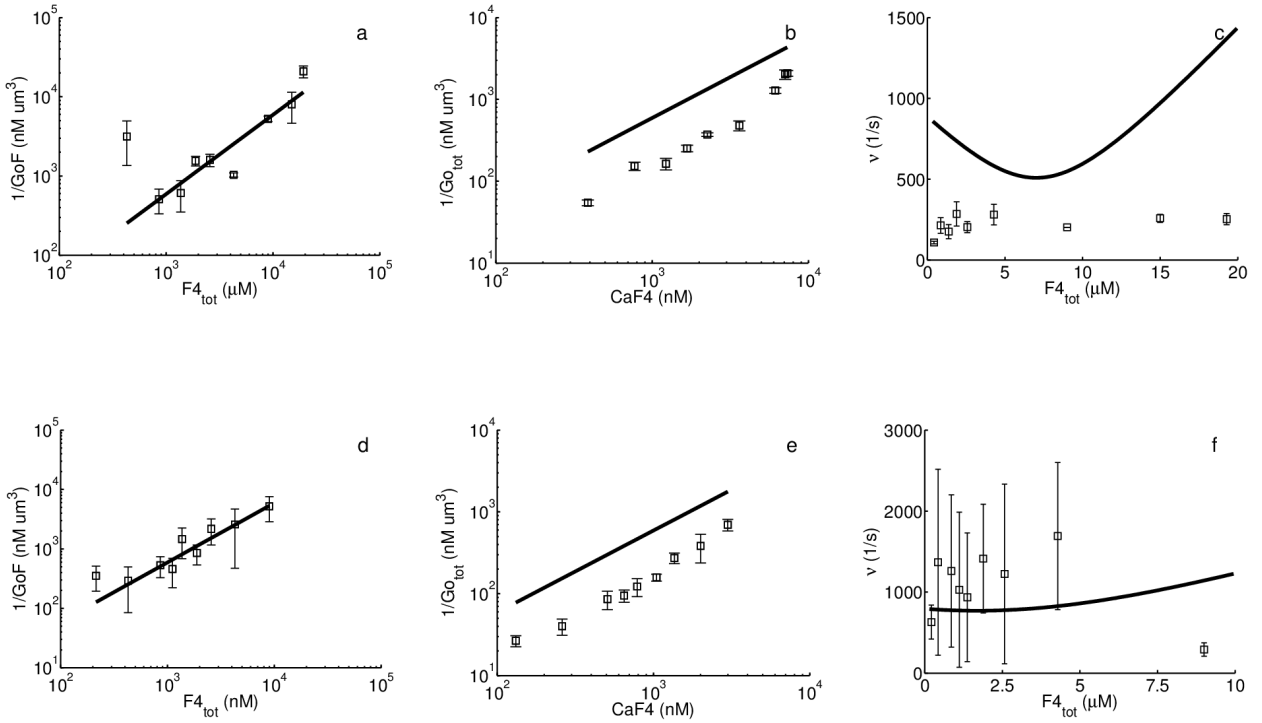


FIG. 2.

Parameters derived from the fitting of the experimental ACFs (with symbols) and theoretical expected values (solid lines). In a logarithmic scale, (left) inverse of the Go_F as function of the total dye concentration used in the solutions, $F4_{tot}$, (middle) inverse of the sum of all the weights, Go_{tot} , as function of the Ca^{2+} -bound dye concentration, CaF_{eq} . CaF_{eq} was estimated theoretically from Eq. (13) with the Ca^{2+} and dye concentrations of the aqueous solutions and K_d given by the manufacturer. (Right) ν as function of the total dye concentration used in the solutions, $F4_{tot}$. (a, b, c) Fluo4 High Affinity and (d, e, f) Fluo4 Low Affinity.

C. Using the theory to determine free diffusion coefficients and reaction rates from the fitting

Being able to identify the parameters of the fitting with those of the theoretical ACF, Eqs. (6)-(9), allowed us to go further and to quantify some relevant parameters of the underlying biophysical model for each aqueous solution, such as the free calcium diffusion coefficient. This entails solving an over-determined problem (7 equations with 6 unknowns). In that sense, we preferred to use the information given by Go_F and Go_{tot} rather than by Go_{ef1} and Go_{ef2} because, as discussed before, these weights carry the largest errors. In particular, knowing D_F , D_{ef1} , D_{ef2} , Go_F , Go_{tot} and ν_F (which we identify with the 7 parameters of the fitting) it is possible to infer the off-rate, k_{off} , of the Ca^{2+} -dye binding reaction, the total concentration of the calcium dye, F_{tot} , the calcium bound dye concentration in equilibrium, CaF_{eq} , and the free diffusion coefficients, D_{Ca} , D_F . We show in Fig. 3 the values of D_{Ca} , D_F and k_{off} obtained as a function of the total dye concentration used in the aqueous solutions, $F_{4_{tot}}$, both for the High Affinity (Figs. 3 (a) - (c)) and the Low Affinity (Figs. 3 (d) - (f)) versions of the dye. Since the solutions only differed in the total amount of dye, all estimated parameter values, with the exception of $F_{4_{tot}}$, should remain approximately constant for all solutions. To estimate the free Ca^{2+} diffusion coefficient the solutions with effective coefficients with large errors or with D_{Ca} far away from the average were discarded (solutions 3, 6, and 10). For Fluo4 High Affinity we obtained $D_{Ca} = (948 \pm 110) \mu m^2/s$, and if we also discard solution 7 which has also a D_{Ca} that is very different from the average, it gives $D_{Ca} = (861 \pm 79) \mu m^2/s$. For Fluo4 Low Affinity we obtained $D_{Ca} = (966 \pm 76) \mu m^2/s$, and if we also discard solutions 12 and 18, that have large errors, we obtained $D_{Ca} = (870 \pm 55) \mu m^2/s$. The average and standard deviation of all estimated biophysical parameters are presented in Table II.

IV. DISCUSSION AND CONCLUSIONS

In this work we have shown how free diffusion coefficients and reaction rates can be quantified in reaction-diffusion systems by performing sets of Fluorescence Correlation Spectroscopy (FCS) experiments and using a biophysical model to interpret the experimental results. In particular, we have applied this approach to the case of Ca^{2+} and a single

wavelength Ca^{2+} dye. To this end we developed the theory that allowed us to derive an approximation of the autocorrelation function of the fluorescence fluctuations (ACF) in the limit of fast reactions. We then performed a series of experiments in solutions containing Ca^{2+} and the Ca^{2+} dye Fluo4 dextran (both High and Low Affinity) with which validated the approach and established its limitations. The analysis of the experiments also allowed us to quantify the transport and reaction properties of two single wavelength Ca^{2+} dyes: High and Low Affinity Fluo4. In doing so we also derived the free diffusion coefficient of Ca^{2+} in aqueous solution. Although this value is already well known ($D_{\text{Ca}} \sim (750\text{-}800) \mu\text{m}^2/\text{s}$ [23], [24]), being able to derive it from the observation of a system in which it is not diffusing freely is quite relevant and provides hints on how to proceed in other settings.

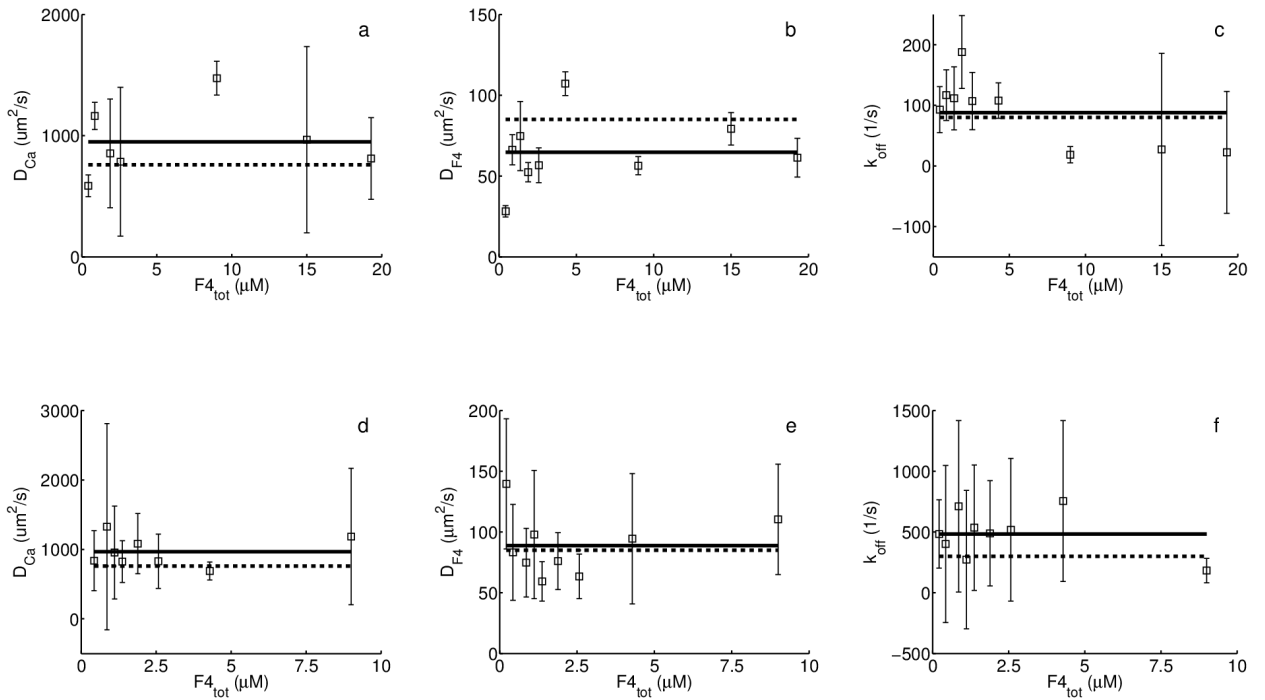


FIG. 3.

Parameters of the underlying biophysical model derived from the fitting parameters for each aqueous solution, D_{Ca} , D_F and k_{off} , (mean and standard deviation over 2-3 experiments with 1 or 2 fits) and average of the values obtained (solid line). (a, b, c) Fluo4 High Affinity and (d, e, f) Fluo4 Low Affinity. In all cases we include the expected values (dashed line) based on the total concentrations used in the solutions and on previous estimates (see text).

TABLE II. Reaction diffusion coefficients estimated from the model. The results are expressed as mean \pm SD.

Parameter	Estimation from the model	Previous estimates
High Affinity Fluo4		
D_F	$(65 \pm 7) \mu m^2/s$	$85 \mu m^2/s$ [22]
D_{Ca}	$(948 \pm 110) \mu m^2/s$	$760 \mu m^2/s$ [23]
k_{off}	$(88 \pm 19) 1/s$	
Low Affinity Fluo4		
D_F	$(89 \pm 8) \mu m^2/s$	$85 \mu m^2/s$ [22]
D_{Ca}	$(966 \pm 76) \mu m^2/s$	$760 \mu m^2/s$ [23]
k_{off}	$(483 \pm 61) 1/s$	

Addressing fundamental problems in Ca^{2+} signaling and Ca^{2+} -dependent cell function calls for the use of multiple approaches. The undeniable need to combine experiments and modeling requires that key biophysical parameters such as the Ca^{2+} diffusion coefficient be quantified *in situ* [25]. Optical techniques are ideal to probe intracellular transport with minimum disruption [26]. Measuring intracellular Ca^{2+} transport in this way, however, is not straightforward because of the multiple interactions of the ions with different cell components [27], [28] and because Ca^{2+} dyes are also Ca^{2+} buffers that alter the ions transport rate [29]. The quantification of diffusion coefficients and reaction constants in such a case requires a careful interpretation of the experimental data in terms of an underlying biophysical model [17]. The work contained in this paper constitutes a necessary first step to advance in this direction.

In this paper, we first focused on the theoretical aspects of the problem. To this end, we derived an analytic approximation for the ACF of a system with Ca^{2+} and a single wavelength dye under the assumption that the Ca^{2+} -dye reaction occurs on a fast timescale, that the free and Ca^{2+} -bound dye molecules diffuse at the same rate and that the former is not fluorescent. The expression obtained, Eqs. (6)-(9), coincides with the one derived in Bismuto et al., 2001 [13]. In particular, we observed that the first two terms in Eq. (6) have the same functional dependence on τ as the only term of Eq. (2) which corresponds to a case with a purely diffusive species. The first term (Eq. (7)) gives $\tau_F = w_r^2/(4D_F)$ that

corresponds to the dye diffusion time across the sampling volume. This term is exact and involves no approximation. The second term (Eq. (8)) has the time scale $\tau_{ef1} = w_r^2/(4D_{ef1})$ and is associated to an effective diffusion coefficient, D_{ef1} , that combines information on diffusion and reactions. D_{ef1} corresponds to the “collective” diffusion coefficient of Pando et al., 2006 [30] which in turn coincides with the effective coefficient determined in the rapid buffering approximation [31]. The last term (Eq. (9)) does not have the functional form of a purely diffusive case, but has an additional exponential factor. Depending on the value of ν_F , it could be neglected to determine τ_F and τ_{ef1} . In the Appendix we presented the results of a thorough analysis of the limitations of this approximation. In particular we computed numerically the “full” ACF (with no approximations) and determined that it could be correctly described by an ACF with the time dependence obtained in the fast reaction limit (Eq. (5)). The fast reaction approximation is always valid for large enough τ , but, as shown in [14] for the case of ‘permanently’ fluorescent molecules, it can still provide a good description of the full ACF for all τ even if the reaction and diffusion times are of the same order. Our results also showed that even if the rapid reaction limit may not hold, fitting the full ACF with an expression of the form Eq. (5) still provides reasonably good estimates of the timescales associated to the free diffusion coefficient of the dye and to the exponentially decaying term. The two effective coefficients given by Eqs. (10) and (11) could also be estimated for certain dye concentrations. The term that corresponds to the free diffusion of the dye (Eq. (7)) is exact. Thus, we can always assume that the weight that corresponds to this timescale is inversely proportional to the total number of dye molecules in the observation volume. The other two individual weights, however, can be incorrectly assessed if the fast reaction approximation is assumed. The total weight, on the other hand, is always inversely proportional to the mean number of Ca^{2+} -bound dye molecules in the observation volume. Thus, in our application of the theory to derive biophysical parameters from the experimental observations we used the total weight and the weight of the term that corresponds to the free diffusion of the dye, but not the other two.

We then performed a series of experiments in solution using Ca^{2+} and Fluo4 High or Low Affinity at various concentrations. Fitting the ACF with an expression of the form of Eq. (5) we obtained the correlation times from which we derived the corresponding diffusion coefficients as functions of the dye concentration. As shown in Fig. 1, one of the coefficients (or, analogously, the correlation time) remained the same for all the concentrations. According

to the theory, this coefficient is to be associated with the free diffusion coefficient of the dye. We observed that the value derived for the dye in its High or Low Affinity version is approximately the same ($D_F = (65 \pm 7) \mu m^2/s$ and $D_F = (89 \pm 8) \mu m^2/s$, respectively). These values are consistent with the value derived in solution for 10kDa tetramethylrhodamine-dextran (TMR-D, $85 \mu m^2/s$) [22]. The variation of the other two coefficients with the dye concentration is particularly visible in the case of the High Affinity version of the dye (Fig. 1 (a)).

We then performed a series of self-consistency checks of our approach. We first compared the relationship between the inverse of the weights, Go_{tot} and Go_F , that we obtained from the experimental fits and the total concentrations of Fluo4 and of Ca^{2+} -bound dye that we used in the solutions with the theoretical expression, Eqs. (16) and (13). The results are shown in Figs. 2 (a) and 2 (d) with symbols for the former and curves for the latter. We can observe in Figs. 2 (a) and 2 (d) that, in the case of the inverse of Go_F versus $F4_{tot}$ relationship, the experimental points match the theoretical prediction. Thus, for these experiments in intact cells we expect to be able to obtain a reliable estimation of the amount of indicator that enters the system. We fitted the experimental points by a linear relationship between the inverse of Go_F and $F4_{tot}$. We obtained $(0.54 \pm 0.08) \mu m^3$ for High Affinity and $(0.56 \pm 0.08) \mu m^3$ for Low Affinity Fluo4. We can observe in Figs. 2 (b) and 2 (e) that, in the case of the inverse of Go_{tot} versus CaF_{eq} relationship, the experimental points lie below the theoretical prediction, as if the actual concentrations of Ca^{2+} -bound dye were smaller than those that can be derived from Eq. (4) using the ones of the solutions and dissociation constant provided by the vendor. If, as before, we fit the experimental points by a relationship between the inverse of Go_{tot} and CaF_{eq} we obtain $(0.23 \pm 0.02) \mu m^3$ for High Affinity and $(0.17 \pm 0.01) \mu m^3$ for Low Affinity Fluo4. The resulting volumes are smaller than the one determined from the calibration, ($V_{ef} = (0.59 \pm 0.1) \mu m^3$), and the mismatch is slightly larger in the case of Low Affinity Fluo4. We must point out that this relationship also depends on the dissociation constant of the Ca^{2+} -dye reaction and that using larger K_d values would decrease the mismatch between the experimental points and the theoretical curve. In order to analyze to what extent the results obtained for both dyes agree with what can be expected theoretically we show in Fig. 4 the ratio of total weights obtained using each dye (weight for High over weight for Low Affinity Fluo4 with symbols) as a function of the total dye concentration for which we had experiments performed with both dyes. We also show in the figure the ratio of Ca^{2+} -bound dye concentrations (Low

over High) computed theoretically using the dissociation constant provided by the vendor. These two ratios should be equal according to Eq. (16). We observe that the ratio determined experimentally is larger than the theoretical one in most cases. This implies that either the experimentally estimated value of CaF_{eq} is underestimated for the High Affinity dye or it is overestimated for the Low Affinity one. We must recall that Eq. (16) holds provided that the fluorescence coming from the free dye molecules is negligible with respect to the one that comes from the Ca^{2+} -bound molecules. Assuming that Eq. (16) holds in a case in which the free dye molecules contribution to the fluorescence is not completely negligible would lead to an overestimation of CaF_{eq} . In such a case the overestimation of CaF_{eq} would be larger for the Low Affinity than for the High Affinity dye. This could explain the difference between the experimental points and the theoretical curve of Fig. 4. This observation together with the fact that the mismatch that can be observed in Fig. 2 is larger for the Low than for the High Affinity Fluo4 makes the latter preferable over the former to study Ca^{2+} transport in other settings. Finally, we also compared the dye concentration dependence of the inverse of the exponential correlation time derived from the experiments (ν) with the one predicted from the theory (ν_F in Eq. (9)) using some estimated parameters as explained before. As expected from the analyses of Fig. 2, it is for the lowest dye concentrations that we obtained comparable results between theory and experiments.

After having tested the self-consistency of our model, we subsequently used it to derive estimates of some biophysical parameters from the parameters of the fitting. More specifically, we obtained the free Ca^{2+} diffusion coefficient, D_{Ca} , and the off-rate of the Ca^{2+} -dye binding reaction, k_{off} . For the former we used the sum of the two effective diffusion coefficients ($D_{ef1} + D_{ef2}$) and subtracted the estimate of the free dye diffusion coefficient, D_F . The values, D_{Ca} and D_F obtained for each solution probed are shown in Fig. 3. The corresponding average values are within the expected range ($D_{Ca}=(861 \pm 79) \mu m^2/s$, $D_F=(65 \pm 7) \mu m^2/s$ in the case of Fluo4 High Affinity and $D_{Ca}=(926 \pm 92) \mu m^2/s$, $D_F=(89 \pm 8) \mu m^2/s$ in the case of Fluo4 Low Affinity). In particular, we obtain consistent values of the free dye diffusion coefficient, D_F , for both the High and Low Affinity version (i.e. $D_F \sim (65-90) \mu m^2/s$) that are of the same order of value as the one estimated for a 10kDa TMR-D [22]. The estimated free Ca^{2+} diffusion are also consistent with what we expected [23], [24].

It is important to note that the values, D_{Ca} and D_F , are derived exclusively from the

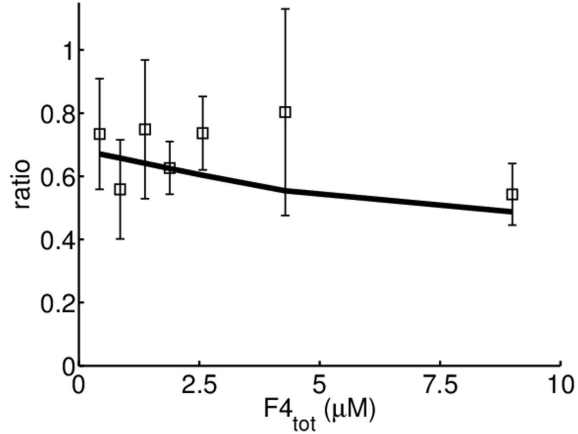


FIG. 4.

Ratio between the total weights, G_{tot} (circles), obtained in experiments with High and Low Affinity Fluo4 and ratio $CaF_{eq}(\text{Low})/CaF_{eq}(\text{High})$, solid line, determined theoretically as functions of the total dye concentration, $F4_{tot}$. The Ca^{2+} -bound dye concentrations were computed using the dissociation constant provided by the vendor.

diffusive correlation times. Thus, these results are not affected by the differences between the Ca^{2+} -bound dye theoretical concentrations, CaF_{eq} , and the ones estimated by the (16) discussed before. In order to obtain k_{off} from the inverse of the exponential correlation time, ν , it is necessary to use concentration estimates. In order to avoid introducing an additional error because of the possible mismatch between the concentrations that we discussed in connection with the differences observed in Fig. 2, to obtain k_{off} from ν we used the estimates of the ratio between the concentrations and the dissociation constant derived from the weight, G_{OF} , of the ACF obtained in the experiments. As discussed before, the values of ν seemed to display the correct behavior only for those solutions with the smallest dye concentrations. In any case, applying the theory to all the experimental results regardless of $F4_{tot}$ gave values of k_{off} within the same order of magnitude (see Figs. 3 (c) and 3 (e)). Using the average of these values we obtained $k_{off} = (88 \pm 19) \text{ s}^{-1}$ and $k_{off} = (483 \pm 61) \text{ s}^{-1}$ for the High and Low Affinity Fluo4, respectively. Using the dissociation constant provided by the manufacturer we derived the on rates. For the High and Low Affinity versions

of the dye, we found similar values ($k_{on} = (0.114 \pm 0.025) \text{ nM}^{-1}\text{s}^{-1}$ and $k_{on} = (0.186 \pm 0.023) \text{ nM}^{-1}\text{s}^{-1}$, respectively). This is consistent with the fact that, in BAPTA (1,2-bis(o-aminophenoxy)ethane-N,N,N',N'-tetraacetic acid) based calcium indicators, increasing K_d values results from an increase in the dissociation rate constant and negligible or only modest decreases in the association rate constants [32], [33]. It is important to note that, while concentrations at equilibrium do not depend on k_{off} and k_{on} , separately, but on $K_d = k_{off}/k_{on}$, their time evolution does. Therefore, the values of k_{off} and k_{on} affect the behavior of the observed signals and knowing them is absolutely necessary to infer the spatio-temporal distribution of free Ca^{2+} from the images [8], [34]. Knowing the free diffusion coefficients of Ca^{2+} and its dyes in the cytosol is necessary as well for this purpose. The values derived in the Results Section, however, correspond to coefficients in aqueous solution. Assuming that the differences in the free diffusion coefficients in solution and in the cytosol are due to differences in viscosity between both media we may assume that the ratio between the free diffusion coefficients of any two substances remains the same in both settings. Thus, by quantifying the rate of diffusion of a molecule that diffuses freely in the cytosol and in solution we can infer the free diffusion coefficient of Ca^{2+} and the dyes in the cytosol as well. We present in the Appendix the results of FCS experiments performed in aqueous solution and in oocytes of *Xenopus laevis* using TMR-D. The ACF can be fitted by an expression of the form Eq. (2), *i.e.*, with a single, free-diffusing component. From the fits we obtained $D_{TMR} = (27 \pm 1) \mu\text{m}^2/\text{s}$ in the cytosol considering that the TMR-D diffusion coefficient in solution is $D_{TMR} = 85 \mu\text{m}^2/\text{s}$ [22], we obtained $D_{TMR-D}(\text{solution})/D_{TMR-D}(\text{oocyte}) \sim 3$.

Assuming that $D_{TMR-D}(\text{solution})/D_{TMR-D}(\text{oocyte}) \sim D_{free}(\text{solution})/D_{free}(\text{oocyte})$, where D_{free} stands for free diffusion coefficient of any substance, we can use the free transport rates of Ca^{2+} and of its dyes in solution to infer their values in the cytosol. We obtain $D_{Ca} \sim (261-313) \mu\text{m}^2/\text{s}$ and $D_F \sim (19-24) \mu\text{m}^2/\text{s}$ starting from the free diffusion coefficients in solution obtained in the experiments performed with High Affinity Fluo4. Thus, the practical implementation presented in this paper not only highlights the advantages of our approach but also allows us to derive information that is key to quantify the free Ca^{2+} distribution that underlies a Ca^{2+} image.

The cytosolic D_{Ca} values derived with our approach are of the same order of magnitude as the one obtained in cytosolic extracts by Allbritton et al., 1992 [5] although the latter ($220 \mu\text{m}^2/\text{s}$) is below our lower bound. The analysis of buffered diffusion of Pando et

al., 2006 [30], showed that the effective diffusion coefficient obtained in the experiments of Allbritton et al, 1992 [5] is the single molecule one and a misinterpretation of its meaning could lead to an underestimation of the actual diffusion rate of Ca^{2+} . This highlights the need of having an underlying biophysical model to interpret transport rates in experiments that do not probe solely free diffusion [17]. The theory and experiments of this paper illustrates this very important point. It also shows how by changing the experimental conditions so that the correlation times associated to effective diffusion change it is possible to identify the latter and quantify concentration-independent biophysical parameters. Other experimentally accessible parameters such as the observation volume can be modified to change some of the correlation times and, in this way, quantify different biophysical parameters [17]. In fact, a comparison of FCS results obtained for different observation volumes has recently been used to quantify the binding rates of transcription factors in single cells of developing mouse embryos [35]. This shows the relevance of performing FCS experiments under different conditions to quantify parameters. The approach presented in this paper can then be extended to address the quantification of transport rates in other biologically relevant reaction-diffusion systems.

ACKNOWLEDGMENTS

We are thankful to Emiliano Perez Ipiña for having provided the code to compute the full ACF and to Lucia Lopez and Estefania Piegari for help with some of experiments. This research has been supported by UBA (UBACyT 20020130100480BA) and ANPCyT (PICT 2013-1301). L.S. and S.P.D. are members of Carrera del Investigador Científico (CONICET).

V. APPENDIX

A. FCS Theory

1. ACF for a system with freely diffusing particles.

When the fluorescence comes solely from a single type of particles, P_f , that diffuse freely with coefficient, D_f , the fluorescence is given by:

$$f(t) = \int QI(r)[P_f](r,t)d^3r \quad (18)$$

where $[P_f](r,t)$ is the particle concentration at time, t , and spatial point, r , the parameter, Q , takes into account the detection efficiency, the fluorescence quantum yield and the absorption cross-section at the wavelength of excitation of the fluorescence. The illumination is commonly approximated by a three-dimensional Gaussian:

$$I(r) = I(0) e^{-\frac{2r^2}{w_r^2}} e^{-\frac{2z^2}{w_z^2}}, \quad (19)$$

with z the spatial coordinate along the beam propagation direction, r a radial coordinate in the perpendicular plane and w_z and w_r the sizes of the beam waist along z and r , respectively. In this case there is an analytic expression for the ACF which is given by Eq. (2). Fitting the ACF obtained from experiments by Eq. (2) two parameters can be determined: Go and the characteristic time τ_f . A previous calibration of the geometric parameters of the sample volume is required in order to obtain D_f from τ_f . This is done performing the same experiments on a sample for which D_f is already known. Once w_r and w_z are determined, the unknown D_f can be estimated from the characteristic time τ_f and P_{tot} from Go .

2. "Full" ACF of a system with Ca^{2+} and a single wavelength dye.

The equations that describe the dynamics of Ca^{2+} and a single wavelength dye, F , that react and diffuse as described in Sec. II are:

$$\frac{\partial[Ca]}{\partial t} = D_{Ca} \nabla^2[Ca] - k_{on}[Ca][F] + k_{off}[CaF] \quad (20)$$

$$\frac{\partial[CaF]}{\partial t} = D_F \nabla^2[CaF] + k_{on}[Ca][F] - k_{off}[CaF] \quad (21)$$

$$\frac{\partial[F]}{\partial t} = D_F \nabla^2[F] - k_{on}[Ca][F] + k_{off}[CaF] \quad (22)$$

In FCS experiments in aqueous solution containing Ca^{2+} and F it is assumed that both species uniformly are distributed and in equilibrium, so that their mean concentrations are given by the equilibrium concentrations Ca_{eq} , F_{eq} and CaF_{eq} , that satisfy Eq. (4) and:

$$CaF_{eq} = \frac{Ca_{eq}F_{tot}}{Ca_{eq} + K_d} \quad (23)$$

$$Ca_{eq} = \frac{1}{2} \left(Ca_{tot} - K_d - F_{tot} + \left((Ca_{tot} - K_d - F_{tot})^2 + 4K_dCa_{tot} \right)^{1/2} \right) \quad (24)$$

$$CaF_{eq} = \frac{1}{2} \left(Ca_{tot} + K_d + F_{tot} - \left((Ca_{tot} - K_d - F_{tot})^2 + 4K_dCa_{tot} \right)^{1/2} \right) \quad (25)$$

In the case in which the calcium indicator is practically non-fluorescent while it is not bound to Ca^{2+} the fluorescence intensity is given by:

$$f(t) = \int QI(r)[CaF](r, t)d^3r, \quad (26)$$

with Q and I as before.

As done in Sigaut et al. 2010 [16], we follow Krischevsky and Bonnet 2002 [36] to determine the spatio-temporal dependence of the fluorescence fluctuations in this case. Namely, the evolution equations (20)-(22) are linearized around the equilibrium solution, Eq. (4). The solution of these linearized equations is then computed in Fourier space and written in terms of branches of eigenvalues, $\lambda(q)$, and eigenvectors, $\chi(q)$, with q the variable in Fourier space (conjugate to the spatial vector (r, z)). The fluorescence fluctuations are then obtained as in Eq. (26) but replacing $[CaF]$ by the corresponding component of the solution of the linearized problem, $\delta[CaF]$. The calculation of the ACF finally assumes that the correlation length of the concentrations at any given time is much smaller than the inter-molecule distance and that the number of molecules obeys Poisson statistics so that its variance and its mean are equal. In this way the ACF, $G(\tau)$, can be written as a sum of as many components as branches of eigenvalues of the linearized problem, in this case:

$$G(\tau) = G_{\lambda_F}(\tau) + G_{\lambda_1}(\tau) + G_{\lambda_2}(\tau) \quad (27)$$

with:

$$G_{\lambda_F}(\tau) = \frac{Go_F}{\left(1 + \frac{\tau}{\tau_F}\right) \sqrt{1 + \frac{\tau}{w^2\tau_F}}} \quad (28)$$

$$G_{\lambda_1}(\tau) = \frac{1}{2(2\pi)^3 h CaF_{eq}} \int d^3q I(q) \left(1 + \frac{(a-h)\nu_F}{(a+h)\Psi(q)} + \frac{(D_{Ca} - D_F)q^2}{\Psi(q)} \right) e^{\lambda_1 t} \quad (29)$$

$$G_{\lambda_2}(\tau) = \frac{1}{2(2\pi)^3 h C_a F_{eq}} \int d^3 q I(q) \left(-1 - \frac{(a-h)\nu_F}{(a+h)\Psi(q)} + \frac{(D_{Ca} - D_F)q^2}{\Psi(q)} \right) e^{\lambda_2 t} \quad (30)$$

where $I(q) = \exp(-(w_r^2 q_r^2 + w_z^2 q_z^2)/4)$, q_r and q_z the Fourier coordinates conjugated to the radial and axial coordinates, r and z , respectively, $a = F_{eq}/K_d$, $h = F_T/F_{eq}$, $\nu_F = k_{off}(a+h)$, $\Psi(q) = \sqrt{(D_F - D_{Ca})^2 q^4 + 2q^2(D_F - D_{Ca})(h-a)k_{off} + (h+a)^2 k_{off}^2}$ and the eigenvalues:

$$\lambda_1 = -\frac{1}{2} (k_{off}(a+h) + (D_F + D_{Ca})q^2) + \frac{\Psi}{2} \quad (31)$$

$$\lambda_2 = -\frac{1}{2} (k_{off}(a+h) + (D_F + D_{Ca})q^2) - \frac{\Psi}{2} \quad (32)$$

3. Approximated ACF of a system with Ca^{2+} and a single wavelength dye.

Although $G_{\lambda_1}(\tau)$ and $G_{\lambda_2}(\tau)$ can be computed numerically, in general there is no analytic algebraic expression for these two components as there is for the one that corresponds to the branch of eigenvalues, $\lambda_F = -D_F q^2$, associated to the free diffusion coefficient of the dye, D_F (see Eq. (28)). As done in Sigaut et al. 2010 [16], however, an analytic expression for $G_{\lambda_1}(\tau)$ and $G_{\lambda_2}(\tau)$ and, consequently, for the ACF can be obtained in the limit of small q which is always valid for long enough times, τ . The approximation is good for almost any value of τ when the observation volume is such that the characteristic reaction time is of the same order or less than the diffusive time across the volume [14]. In fact, if we expand the integrands that define $G_2(\tau)$ and $G_3(\tau)$ in powers of q and keep the expansion up to $O(q^2)$ we obtain Eq. (6) This limit is valid provided that the reactions occur on a faster timescale than diffusion across the observation volume, i.e., if $\tau_{reac} \equiv (k_{off} + k_{on}(Ca_{eq} + F_{eq}))^{-1} \ll w_\tau^2/(4D_{Ca})$.

B. Limits of applicability of the fast reaction approximation

In order to study when the fast reaction approximation of the ACF can be used to estimate different biophysical parameters we computed numerically the full ACF, $G(\tau)$, given by Eqs. (27)-(30) using an adaptive Lobatto quadrature algorithm, with the *quadl* function on the MatLab platform (The MathWorks, Natick, MA) and the parameters listed in Table III. We compared the results of these computations with the approximated ACF, $G_{approx}(\tau)$,

TABLE III. Parameters used to compute the full and approximated ACFs numerically. For the concentrations of dye we tried the values listed in Table I.

Parameter	Value	
w_r	0.28 μm	
w	5	
D_{Ca}	760 $\mu m^2/s$	
D_F	85 $\mu m^2/s$	
Ca_{tot}	4285 nM	
	High Affinity Fluo4	Low Affinity Fluo4
K_d	772 nM	2600 nM
k_{off}	80 s^{-1}	300 s^{-1}

given by Eqs. (6) - (9) using the same parameters. For the comparison we computed the difference between both functions given by:

$$\varepsilon^2 = \frac{1}{n} \sum_{i=1}^n (G(\tau_i) - G_{approx}(\tau_i))^2 \quad (33)$$

with n the total number of data points. For the lowest dye concentrations considered $G(\tau)$ and $G_{approx}(\tau)$ were indistinguishable. As the concentration of dye was increased, the difference between the full and the approximated ACF's first increased, with $G_{approx}(\tau)$ decaying at an earlier correlation time than $G(\tau)$. The difference between $G(\tau)$ and $G_{approx}(\tau)$ reached a maximum at $F4_{tot} \sim 4 \mu M$. Further increments in $F4_{tot}$ decreased this difference. This is illustrated in Fig. 5 where we show $G(\tau)$ and $G_{approx}(\tau)$ with solid and dashed lines, respectively, for $F4_{tot}=429 nM$, 7500 nM , 15 μM using the parameters of Fluo4 High Affinity. Similar results are obtained for Fluo4 Low Affinity (data not shown). The difference between the two ACF's, however, is never significantly large: we obtained $2.31 \times 10^{-9} \leq \varepsilon^2 \leq 1.17 \times 10^{-8}$ for High Affinity Fluo4 and $1.55 \times 10^{-8} \leq \varepsilon^2 \leq 4.11 \times 10^{-8}$ for Low Affinity Fluo4. The differences between the individual components associated to τ_{ef1} and τ_{ef2} are much larger.

We then analyzed what correlation times could be derived by fitting the full ACF with Eq. (5). We probed two options. First, we fixed the timescales as in the fast reaction approximation and fitted the weights. Secondly, we fitted both the weights and the timescales.

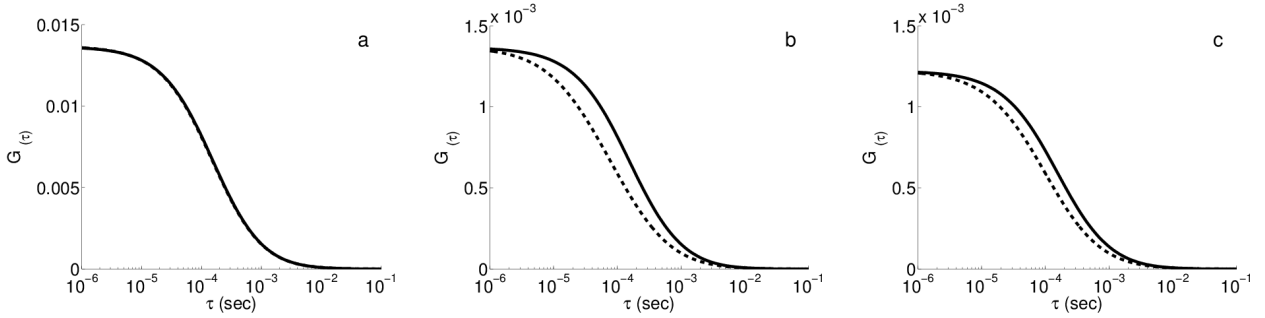


FIG. 5.

Full (solid line, Eqs. (27)-(30)) and approximated (dashed line, Eqs. (6)-(9)) ACF's for Fluo4 High Affinity using the parameters listed in Table III. $F4_{tot} = 429$ nM (a), 7500 nM (b), $15 \mu M$ (c).

From the second test we determined that the fitted values obtained for τ_0 were similar to those prescribed by the fast reaction approximation, τ_F , for all dye concentrations. The fitted values of $1/\nu$ were similar to the values of the fast reaction approximation for dye concentrations below $4.826 \mu M$. For higher dye concentrations the fitted values of $1/\nu$ for High Affinity Fluo4 followed the same pattern and stayed within the same order of magnitude as the value of the fast reaction approximation although it got three times the approximated value at $F4_{tot} = 12 \mu M$. For Low Affinity Fluo4 the variations of $1/\nu$ with $F4_{tot}$ were slightly different but $1/\nu$ stayed within the fast reaction approximation values for all dye concentrations becoming between twice and three times smaller at $F4_{tot} = 15 \mu M$. For all dye concentrations we obtained $\tau_0 = \tau_F$ and $G_1 \ll G_0$ and for dye concentration below $8.25 \mu M$ we obtained $\tau_2 \approx \tau_0$. These results are illustrated in Figs. 6 (a) - (b) where we show the ratios τ_0/τ_F , τ_2/τ_{ef2} , ν_F/ν , between the fitted values and those of the fast reaction approximation and G_1/G_0 , as a function of $F4_{tot}$ for High Affinity (Fig. 6 (a)) and Low Affinity (Fig. 6 (b)) Fluo4. From the test we determined that the full ACF could be approximated fairly well using the expression given by Eq. (5), with the timescales of the fast reaction approximation but with slightly different weights. This is illustrated in Fig. 6 (c) where we have plotted these two ACF's for High Affinity Fluo4 at $F4_{tot} = 7500$ nM. Similar figures are obtained for Low Affinity Fluo4 and at other dye concentrations (data not shown). In this case the mismatch, ε^2 , obtained ranged between 7.2×10^{-12} and 1.57×10^{-10}

for High Affinity and between 9.69×10^{-11} and 2.46×10^{-9} for Low Affinity Fluo4. Regarding the individual components of the fitted ACF, the weights obtained, G_0 , G_2 , were of the same order of magnitude as those of the fast reaction approximation, G_{oF} , G_{oef2} , and G_1 was negligible for low dye concentrations. This is illustrated in Fig. 6 (d) where we have plotted the ratios between the fitted and the fast reaction approximation weights, G_0/G_{oF} , G_1/G_{oef1} , G_2/G_{oef2} , as a function of $F4_{tot}$ for Fluo4 High Affinity. Similar patterns are observed for Fluo4 Low Affinity (data not shown).

C. FCS experiments in aqueous solution and in *Xenopus laevis* oocytes with tetramethylrhodamine-dextran to determine the factor by which free diffusion coefficients are rescaled in the cytoplasm.

We here present the results of performing FCS experiments with tetramethylrhodamine-dextran (TMR-D) in aqueous solution and in *Xenopus laevis* oocytes. The aim of these experiments is to determine the conversion factor between free diffusion coefficients in the two media.

X. laevis oocytes, previously treated with collagenase and stored in Barth's solution, were loaded with 37 nl of TMR-D at different concentrations. Intracellular microinjections were performed using a Drummond microinjector. Assuming a 1 μ l cytosolic volume, the final concentration of TMR-D was 0.9, 1.1, 1.4 or 1.85 μ M. FCS measurements were performed on a spectral confocal scanning microscope FluoView 1000 (Olympus, Tokyo, Japan), employing a 60x, 1.35 N.A. oil-immersion objective (UPlanSAPO, Olympus) and a pinhole aperture of 115 μ m. Single point measurements at a 50 kHz sampling rate were performed for a total duration of 167 s (equivalently, 8365312 data points) employing a 543 nm line and detecting the fluorescence in the range (555-655) nm. For the aqueous solutions the measurements was performed at ~ 20 μ m from the coverslip and for the oocytes, at the cortical granules region in the animal hemisphere. Experimental ACF's were calculated with a custom-made routine written on the Matlab platform [20]. To this end, each 167 s long record was divided into $N_{sol}=1021$, 164 ms long segments containing 2^{13} points each for the experiments in aqueous solutions and into $N_{oo}=510$, 328 ms long segments containing 2^{14} points each for the experiments in *X. laevis* oocytes. The ACF was computed for each of the $N_{sol}=1021$ or $N_{oo}=510$ segments from which the average ACF was obtained. As the confocal volume

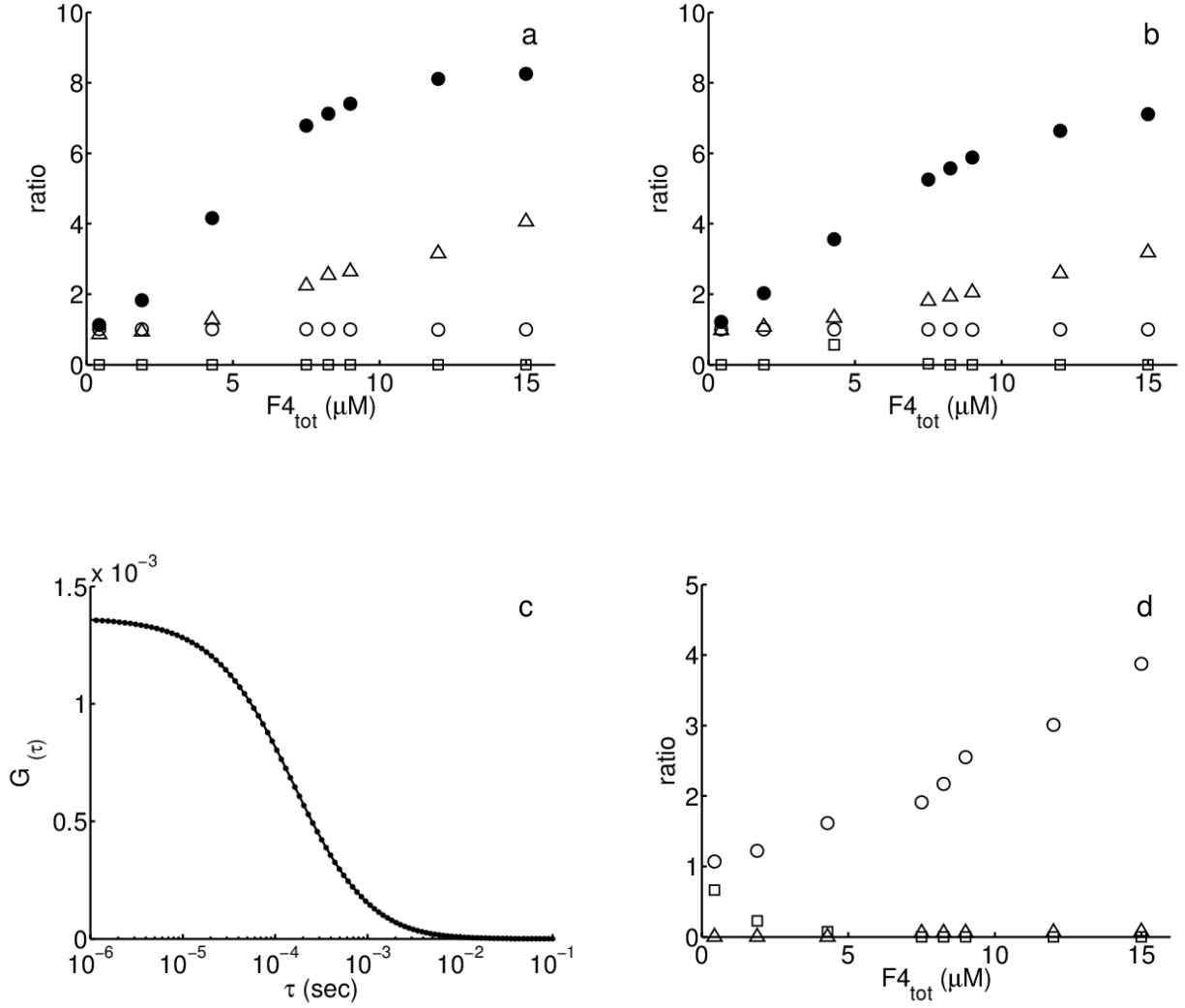


FIG. 6.

Ratios τ_0/τ_F (white circles), τ_2/τ_{ef2} (black circles), ν_F/ν (triangles) between the fitted values and those of the fast reaction approximation and G_1/G_0 (squares), as a function of $F4_{tot}$ for High Affinity (a) and Low Affinity (b) Fluo4. (c) Full ACF (dotted line) fitted with Eq. (5), fixing the timescales (solid line) for $F4_{tot}=7500\text{nM}$. (d) Ratios between the fitted weights with the timescales fixed and the fast reaction approximation weights, G_0/G_{oF} (circles), G_1/G_{oef1} (triangles), G_{o2}/G_{oef2} (squares), as a function of $F4_{tot}$ for Fluo4 High Affinity.

dimensions are wavelength-dependent we used the FCS experiments with TMR-D in solution

to estimate the beam waist and aspect ratio at 543 nm. Assuming a diffusion coefficient of $D_{TMR-D} = 85 \mu m^2/s$ [22] we obtained $w_r = (0.199 \pm 0.003) \mu m$ and $w = wz/wr = 5$. The ACF was fitted using only one (diffusive) component as in Eq. (2).

We show in Fig. 7 the ACF obtained from FCS experiments performed in *X. laevis* oocytes with TMR-D (Fig. 7 (a)). Using Eq. (2) to fit the data of Fig. 7 we obtain $D_{TMR}(oocyte) = (27 \pm 1) \mu m^2/s$. The TMR-D diffusion coefficient in solution is $D_{TMR}(solution) = 85 \mu m^2/s$ [22]. Thus, it is $D_{TMR-D}(oocyte)/D_{TMR-D}(solution) \sim 3$.

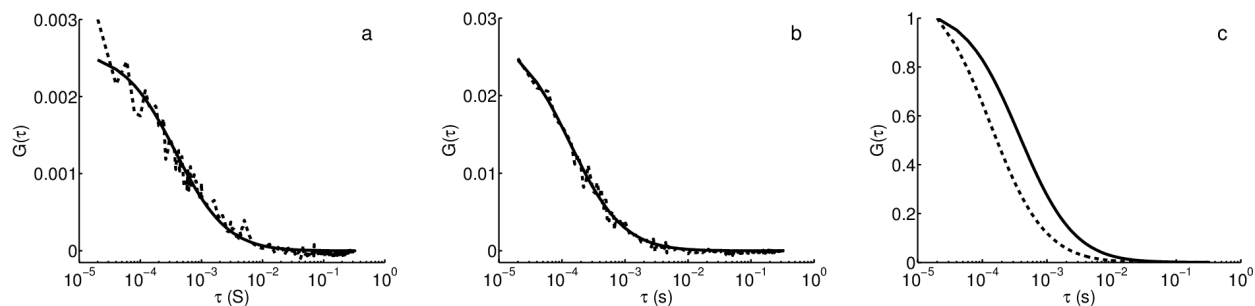


FIG. 7.

- (a) ACF obtained from FCS experiments performed in *X. laevis* oocytes microinjected with 37 nl of TMR-D = 30 μM (dashed line) fitted by Eq. (2) (solid line). (b) As in (a) for solution of TMR-D = 50 nM. (c) ACF's from the fits performed in (a) and (b) (solid and dashed line, respectively), normalized.

REFERENCES

- [1] S. L. Dargan and I. Parker, J Physiol **553**, 775 (2003).
- [2] S. L. Dargan, B. Schwaller, and I. Parker, The Journal of Physiology **556**, 447 (2004), ISSN 1469-7793.
- [3] M. Nelson, H. Cheng, M. Rubart, L. F. Santana, et al., Science **270**, 633 (1995).
- [4] X.-P. Sun, N. Callamaras, J. S. Marchant, and I. Parker, J Physiol (Lond) **509**, 67 (1998).
- [5] N. Allbritton, T. Meyer, and L. Stryer, Science **258**, 18121815 (1992).

- [6] R. M. Paredes, J. C. Etzler, L. T. Watts, W. Zheng, and J. D. Lechleiter, *Methods* **46**, 143 (2008).
- [7] E. Piegari, L. Lopez, E. P. Ipiña, and S. P. Dawson, *PloS one* **9**, e95860 (2014).
- [8] L. Bruno, G. Solovey, A. C. Ventura, S. Dargan, and S. Ponce Dawson, *Cell Calcium* p. in press (2010).
- [9] E. L. Elson, *Biophysical journal* **101**, 2855 (2011).
- [10] D. Magde, E. Elson, and W. W. Webb, *Phys. Rev. Lett.* **29**, 705 (1972).
- [11] E. L. Elson, *Traffic* **2**, 789 (2001).
- [12] E. Haustein and P. Schwille, *Annual Review of Biophysics and Biomolecular Structure* **36**, 151 (2007).
- [13] E. Bismuto, E. Gratton, and D. C. Lamb, *Biophys. J.* **81**, 3510 (2001).
- [14] E. P. Ipiña and S. P. Dawson, *Phys. Rev. E* **87**, 022706 (2013).
- [15] E. P. Ipiña and S. P. Dawson, *Biophys. J.* **107**, 2674 (2014).
- [16] L. Sigaut, M. L. Ponce, A. Colman-Lerner, and S. P. Dawson, *Phys. Rev. E* **82**, 051912 (2010).
- [17] L. Sigaut, J. E. Pearson, A. Colman-Lerner, and S. Ponce Dawson, *PLoS Comput Biol* **10**, e1003629 (2014).
- [18] A. Abu-Arish, A. Porcher, A. Czerwonka, N. Dostatni, and C. Fradin, *Biophysical Journal* **99**, L33 (2010).
- [19] T. Gregor, T., W. D.W., and W. E.F., Bialek, *Cell* **130**, 153 (2007).
- [20] MATLAB, *version 7.10.0 (R2010a)* (The MathWorks Inc., Natick, Massachusetts, 2010).
- [21] C. T. Culbertson, S. C. Jacobson, and J. M. Ramsey, *Talanta* **56**, 365 (2002), ISSN 0039-9140.
- [22] A. Gennerich and D. Schild, *Biophysical Journal* **83**, 510 (2002), ISSN 0006-3495.
- [23] D. Qin, A. Yoshida, and A. Noma, *Japanese Journal of Physiology* **41**, 333 (1991).
- [24] W. M. Haynes, *CRC Handbook of Chemistry and Physics 2015-2016*, CRC Handbook of Chemistry and Physics (CRC Press, 2015), 96th ed., ISBN 1482260964,9781482260960.
- [25] F. von Wegner, N. Wieder, and R. H. Fink, *Frontiers in genetics* **5**, 376 (2014).
- [26] M. Wachsmuth, C. Conrad, J. Bulkescher, B. Koch, R. Mahen, M. Isokane, R. Pepperkok, and J. Ellenberg, *Nature biotechnology* **33**, 384 (2015).
- [27] A. Biess, E. Korkotian, and D. Holcman, *PLoS Comput Biol* **7**, e1002182 (2011).
- [28] P. C. Bressloff and J. M. Newby, *Reviews of Modern Physics* **85**, 135 (2013).
- [29] E. Piegari, L. Sigaut, and S. P. Dawson, *Cell calcium* **57**, 109 (2015).

- [30] B. Pando, S. P. Dawson, D.-O. D. Mak, and J. E. Pearson, Proceedings of the National Academy of Sciences **103**, 5338 (2006).
- [31] G. D. Smith, J. Wagner, and J. Keizer, Biophysical Journal **70**, 2527 (1996).
- [32] R. Y. Tsien, Calcium as a cellular regulator pp. 28–54 (1999).
- [33] M. Naraghi, Cell Calcium **22**, 255 (1997), ISSN 0143-4160.
- [34] A. C. Ventura, L. Bruno, A. Demuro, I. Parker, and S. Ponce Dawson, Biophys. J. **88**, 2403 (2005).
- [35] M. D. White, J. F. Angiolini, Y. D. Alvarez, G. Kaur, Z. W. Zhao, E. Mocskos, L. Bruno, S. Bissiere, V. Levi, and N. Plachta, Cell **165**, 75 (2016).
- [36] O. Krichevsky and G. Bonnet, Reports on Progress in Physics **65**, 251 (2002).